



HAL
open science

An early comparison of nano to microplastic mass in a remote catchment's atmospheric deposition

Steve Allen, Dušan Materić, Deonie Allen, Anna Macdonald, Rupert Holzinger, G. Le Roux, Vernon Phoenix

► To cite this version:

Steve Allen, Dušan Materić, Deonie Allen, Anna Macdonald, Rupert Holzinger, et al.. An early comparison of nano to microplastic mass in a remote catchment's atmospheric deposition. *Journal of Hazardous Materials Advances*, 2022, 7, pp.100104. 10.1016/j.hazadv.2022.100104 . hal-03764527

HAL Id: hal-03764527

<https://hal.science/hal-03764527>

Submitted on 16 Nov 2022

HAL is a multi-disciplinary open access archive for the deposit and dissemination of scientific research documents, whether they are published or not. The documents may come from teaching and research institutions in France or abroad, or from public or private research centers.

L'archive ouverte pluridisciplinaire **HAL**, est destinée au dépôt et à la diffusion de documents scientifiques de niveau recherche, publiés ou non, émanant des établissements d'enseignement et de recherche français ou étrangers, des laboratoires publics ou privés.

An early comparison of nano to microplastic mass in a remote catchment's atmospheric deposition

Steve Allen^{1,3,4*}, Dušan Materić², Deonie Allen^{3,4}, Anna MacDonald³, Rupert Holzinger², Gael Le Roux⁴, Vernon R Phoenix³

¹Department of Earth and Environmental Sciences, Dalhousie University, Halifax, Canada

²Utrecht University, Institute for Marine and Atmospheric research Utrecht (IMAU), Utrecht, The Netherlands

³Department of Civil and Environmental Engineering, University of Strathclyde, Glasgow, Scotland

⁴Laboratoire écologie fonctionnelle et environnement, Université de Toulouse, CNRS, Toulouse, France. 3

*Corresponding author (st504087@dal.ca)

CRedit authorship contribution statement

Steve Allen, Dušan Materić: Conceptualization, Resources, Methodology, Data curation, Investigation, Writing – original draft, Writing – review & editing. **Deonie Allen:** Resources, Methodology, Data curation, Investigation, Writing – original draft, Writing – review & editing. **Anna MacDonald:** Data curation, Writing – original draft, Writing – review & editing. **Vernon R Phoenix, Gael Le Roux, Rupert Holzinger:** Resources, Writing – review & editing.

1 An early comparison of nano to microplastic mass in a remote catchment's 2 atmospheric deposition

4 Abstract

5 The existence of nano sized plastic (NP) has been discussed heavily in recent years, however
6 physical proof from environmental samples and direct comparisons to characterized
7 microplastics is limited. Here we compare microplastic (MP) particles and counts (>10µm) to
8 NP particle (<0.45µm) mass concentrations from deposition at a remote field site in the French
9 Pyrenees (elevation 1425 m a.g.l.). Using Thermal Desorption – Proton Transfer Reaction –
10 Mass Spectrometry (TD-PTR-MS) analysis, the data shows that NP is present in atmospheric
11 deposition in quantities up to 2.0×10^5 nanograms $m^{-2} day^{-1}$, comparable to that of the >10µm
12 microplastic (up to 1.1×10^5 nanograms $m^{-2} day^{-1}$). This comparison indicates the quantity of
13 NP and MP may be similar in this atmospheric deposition, however the estimated particle
14 count for NP is understandably multiple orders of magnitude greater compared to MP.
15 Backward trajectory modelling was used to consider the transport of these MP and NP
16 particles. This highlighted the extended spatial influence of NP and its propensity to remain
17 elevated over a 7-day period.

18 **Keywords:** aerosol pollutants, transport processes, microplastics, nanoplastics, TD-PTR-
19 MS

21 Introduction

22 The issues surrounding plastic pollution are currently receiving multidisciplinary attention, with
23 its discovery in all environmental matrices and in some of the most remote locations (for
24 example, the Arctic, Antarctic, Alps and Ecuadorian Andes)(S. Allen et al., 2021; Ambrosini et
25 al., 2019; Bergmann et al., 2019; Brahney et al., 2020; Cabrera et al., 2020; Huntington et al.,
26 2020; Kim et al., 2021; Materic et al., 2022). While research has focused on finding, quantifying
27 and assessing the environmental impact of microplastics (MP, 1µm-5mm plastic particles),
28 there is a growing interest in nanoplastic occurrence in the environment.

29 Nanoplastics have been describes as plastic particles smaller than 1 µm and also confusingly
30 as particles smaller than 100 nm. The definition of nano has meaning when applied to materials
31 below 100 nm if that material behaves differently to its larger counterparts(Joachim, 2005).
32 This is the level at which many materials start to exhibit Brownian motion(Feynman, 1963) as
33 it bounces off molecules it is in suspension with. As both diffuse and ballistic Brownian motion
34 are known to occur in particles up to 2.5 µm (Silica) in air, the term nano encompasses the
35 small particle sizes in this study (T. Li & Raizen, 2013). Whist it is acknowledged that 100 nm
36 is a practical limit for the safety regulations of industry, it is widely accepted among the plastic
37 pollution research community that sub-micron synthetic polymer material should be described
38 as nanoplastic (NP are particles <1µm) (Frias & Nash, 2019; Gigault et al., 2021). This simpler
39 definition being easier for policy makers and the general public to understand without having
40 to further explain the definition. With this in mind, the definition of NP used in this study is 1
41 nm-1µm.

42 Nanoplastic particles form an important element in the global plastic cycle and plastic pollution
43 impact (D. Allen et al., 2022; Mitrano et al., 2021). NP occur as primary (designed as nano
44 sized plastic particles) or secondary (larger particles degraded to nano size) and have been
45 found in the marine waters (Gonçalves & Bebianno, 2021; Piccardo et al., 2020), soil (Wahl et

46 al., 2021), air (Materić et al., 2021) and biota (Ferreira et al., 2019). NP can be more easily
47 taken up (ingested, inhaled or adsorbed) by biota due their small size (Banerjee & Shelver,
48 2021), entering the ecosystem. Due to the small size and often jagged shape, secondary NP
49 (and small MP) can pass through or impact on epithelial membranes and early studies suggest
50 there may be a link between changed function, immune compromission and cytotoxicity
51 (Bergmann et al., 2015; Deng et al., 2020; Huang et al., 2020; B. Li et al., 2020; Liu et al.,
52 2020; H. Yang et al., 2020). As a result, NP could potentially influence the cellular to organism
53 functionality, a concern to both environmental and human health (Banerjee & Shelver, 2021;
54 Rubio et al., 2020; Wright & Kelly, 2017; Yee et al., 2021). Given this risk, understanding the
55 extend of MP and NP pollution is crucial. The ratio of MP to NP is still generally hypothesised,
56 with limited data to directly compare MP to NP within individual samples. Formative studies
57 indicate notable atmospheric NP mass (in snow and dry atmospheric deposition) 42 (+32/-25)
58 kg km⁻² year⁻¹ (Materić et al., 2021) and 13.2-52.3 ng ml⁻¹ (in ice)(Materic et al., 2022).

59 Nano sized plastics (NP, 1 nm-1µm) have been difficult to assess in environmental matrices
60 due to their small size (published and functional limitations of spectroscopy are approximately
61 µRaman-1µm and FTIR-10µm) (Xu et al., 2019; Zheng et al., 2021) and environmental
62 concentrations (for example, Py-GCMS limit of quantification for is µg's rather than
63 ng)(Akoueson et al., 2021; Okoffo et al., 2020). The vast majority of studies assessing NP
64 have thus far have been theoretical or laboratory based, providing a limited understanding of
65 the possible quantities in the environment. However, recent research from Materić et al.
66 (Materic et al., 2022; Materić et al., 2020, 2021) illustrates the effective use of Thermal
67 Desorption – Proton Transfer Reaction – Mass Spectrometry (TD-PTR-MS) for environmental
68 NP analysis. The use of this new method has paved the way for analysis of the elusive
69 nanoplastics in environmental samples.

70 **Materials and Methods**

71 Atmospheric deposition samples were collected from the remote mountain location of
72 Bernadouze, a long-term monitoring station in the central Pyrenees, France (42° 48' 14.6" N,
73 1° 25' 06.8" E, 1,425 m above mean sea level). Standard total atmospheric deposition
74 collectors were used over the course of 5 months, November to March 2018, to collect monthly
75 cumulative wet and dry deposition (sample time steps were constrained by access due to
76 snow closure of the access road) (Sample durations: November – 12 days, December – 19
77 days, January – 34 days, February – 41 days, March – 34 days). Samples were collected as
78 total atmospheric deposition (wet + dry deposition) using a Palmex Rain Sampler (sampling
79 area of 0.014 m², open diameter of 135 mm) and a NILU Particle Fallout Collector (sampling
80 area of 0.03 m², open diameter of 22 mm). Atmospheric deposition collectors were open for
81 the full sampling period and acted as duplicate sample sets. Multiple field full process blanks
82 were collected on site during this sampling period (November – March 2018). Sample
83 collectors were rinsed thoroughly on site (3 times, approximately 250ml) with MilliQ water and
84 the sample was decanted into sterilised glass containers (including the equivalent field blanks)
85 and transported back to the laboratory where they were stored in a temperature controlled,
86 dark, fridge (4 degrees) until sample preparation and analysis (S. Allen et al., 2019).

87 Samples were pre-filtered through a 0.45µm pore 47mm diameter polytetrafluoroethylene
88 (PTFE) filters that had been pre-flushed using filtered MilliQ water (250ml MilliQ flush)(Materić
89 et al., 2020). The filtrate was placed in sterilised 25ml glass vial for TD-PTR-MS analysis (vials
90 prepared by heating to 400°C overnight, sterilised containers were wrapped in sterilised
91 aluminium foil after heading to minimise external contamination). No sample pre-treatment
92 was undertaken. The remaining material on the PTFE filter was then flushed with H₂O₂ (30%
93 w/w) into covered, sterilised borosilicate glass test tubes in a dry heat block at 50°C to

94 complete organic digestion(S. Allen et al., 2019). After organic material was adequately
1 95 removed the sample was filtered onto pre-flushed PTFE filters to remove residual H₂O₂ and
2 96 liquid and then flushed into sterilised glass density separation tubes with ZnCl₂ (1.6 g ml⁻¹
3 97 density) and agitated to aid MP separation from mineral and residual organic material(S. Allen
4 98 et al., 2019). Settled material was removed from the bottom of the density separation tubes
5 99 and the remaining upper liquid plus microplastic material was filtered onto 25mm diameter
6 100 aluminium oxide (Whatman Anodisc) filters for μ Raman analysis.
7 101

8 102 The samples were analysed for MP by μ Raman spectroscopy (785nm laser, 1200 l/mm
9 103 grating, scanning 200-2000cm⁻¹ with 15s acquisition time and 10 accumulations) and Nile Red
10 104 fluorescence to quantitatively characterise the atmospheric deposition of MP at this site for
11 105 this monitoring period (S. Allen et al., 2019). Raman spectra analysis was undertaken using
12 106 open source Spectragryph software and available databases(Menges, 2018; Munno et al.,
13 107 2020; Primpke et al., 2020). The limits of quantification for μ Raman analysis for these samples
14 108 was set to 10 μ m.
15 109

16 110 NP analysis was completed as a blind test by Thermal Desorption – Proton Transfer Reaction
17 111 – Mass Spectrometry followed protocols previously developed by Materic et al. (2020)(Materić
18 112 et al., 2020) herein briefly described. TD-PTR-MS is a destructive analytical method, similar
19 113 to Py-GCMS, but can be used for nanoplastic analysis in line with microplastic assessment.
20 114 Filtered (<0.45 μ m) samples were well mixed (shaken but not vortexed to ensure sample
21 115 particle integrity) to ensure homogeneity throughout the sample, then sub-sampled into three
22 116 0.5ml replicates that were individually analysed by TD-PTR-MS (PTR-MS model PTR8000,
23 117 IONICON Analytik, Austria) directly via sterilised glass vials (10ml) (Materić et al., 2020). Field
24 118 blanks were analysed in the same way and used to blank correct all results. Process blanks
25 119 were carried out using MilliQ water and underwent the same procedures and durations as the
26 120 samples and quantities subtracted from final results (see supplementary information). The TD-
27 121 PTR-MS analysis of NP was undertaken using the fingerprinting algorithms created and
28 122 published in Materic et al. (Materic et al., 2022; Materić et al., 2020, 2021).
29 123

30 124 All samples and field blanks were transported to the laboratory where sample preparation
31 125 occurred in a clean and access-controlled space. Cotton clothing and lab coats were worn to
32 126 minimise sample contamination and laboratory surfaces were cleaned and covered with non-
33 127 plastic material (sterilised aluminium foil). Field blanks were processed following the same
34 128 procedures (full process blanks) (S. Allen et al., 2019) and counts subtracted from the final
35 129 results (counts in supplementary).
36 130

37 131 **Results and Discussion**

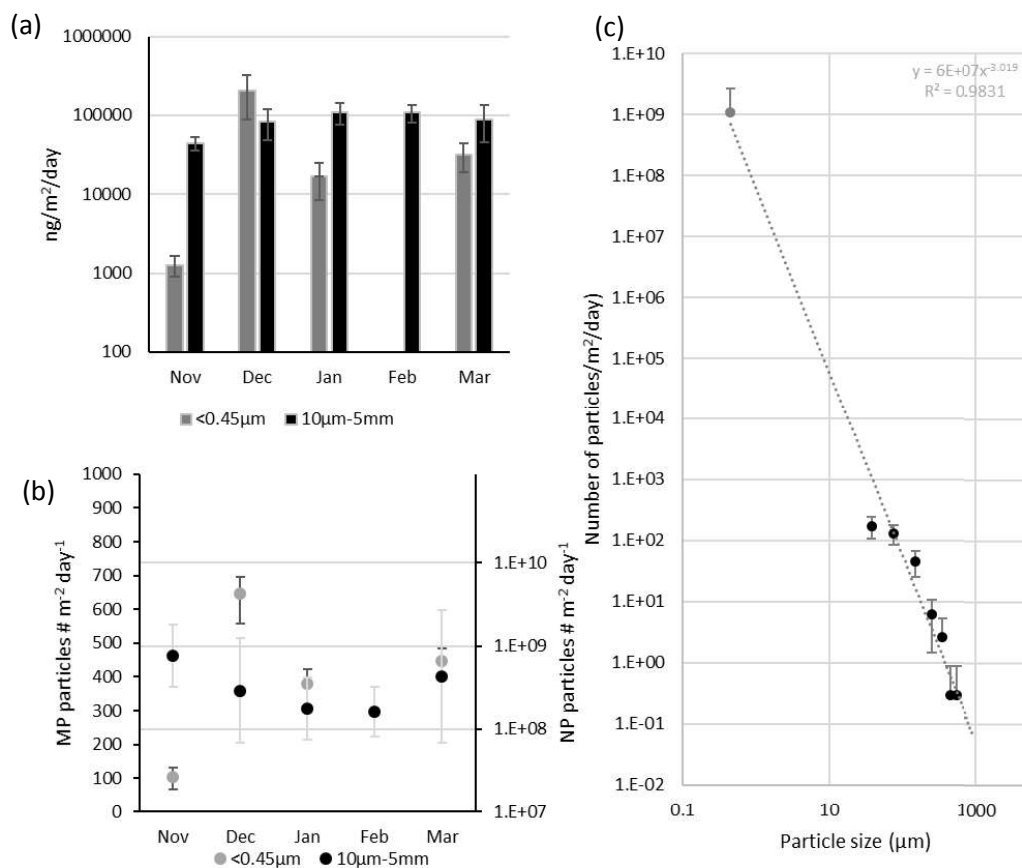
38 132 *MP and NP quantitative characterisation*

39 133 The μ Raman analysed MP particle counts and polymer types and the TD-PTR-MS analysed
40 134 NP mass and polymer types were compared by calculating the respective mass and particle
41 135 counts for each sample (see Supplementary Information and data for additional details). MP
42 136 results were converted from polymer type and particle count to mass relative to their particle
43 137 size following, with results presented relative to particle size (Figure 1c) and to all MP in each
44 138 sample (>10 μ m) (Figure 1a). Similarly, the NP mass relative to polymer type (<0.45 μ m) were
45 139 converted to particle counts (assuming a spherical conservative particle size of 0.45 μ m) to
46 140 enable direct comparison to the MP particle counts (Figure 1b, c).
47 141

48 142 The total deposited MP >10 μ m mass ranged between 44 x10³ - 109 x10³ ng m⁻² day⁻¹ with an
49 143 overall average for the monitoring period of 87 x10³ ng m⁻² day⁻¹. Comparably, total NP
50 144 <0.45 μ m mass ranged from below detection to 203 x10³ ng m⁻² day⁻¹, with an average NP
51 145 mass for the monitoring period of 50 x10³ ng m⁻² day⁻¹. The mass of MP >10 μ m and NP
52 146
53 147
54 148
55 149
56 150
57 151
58 152
59 153
60 154
61 155
62 156
63 157
64 158
65 159

141 <0.45µm deposited at this location for this period is comparable (average results and range
 142 are within an order of magnitude) and are in agreement with the simulated NP fibre and MP
 143 release experiment findings of T. Yang et al., 2021. The NP mass results (18 (+55/-17) kg km⁻²
 144 year⁻¹) are also comparable to previously published results, 42 (+32/-25) kg km⁻² year⁻¹
 145 (Materić et al., 2021).

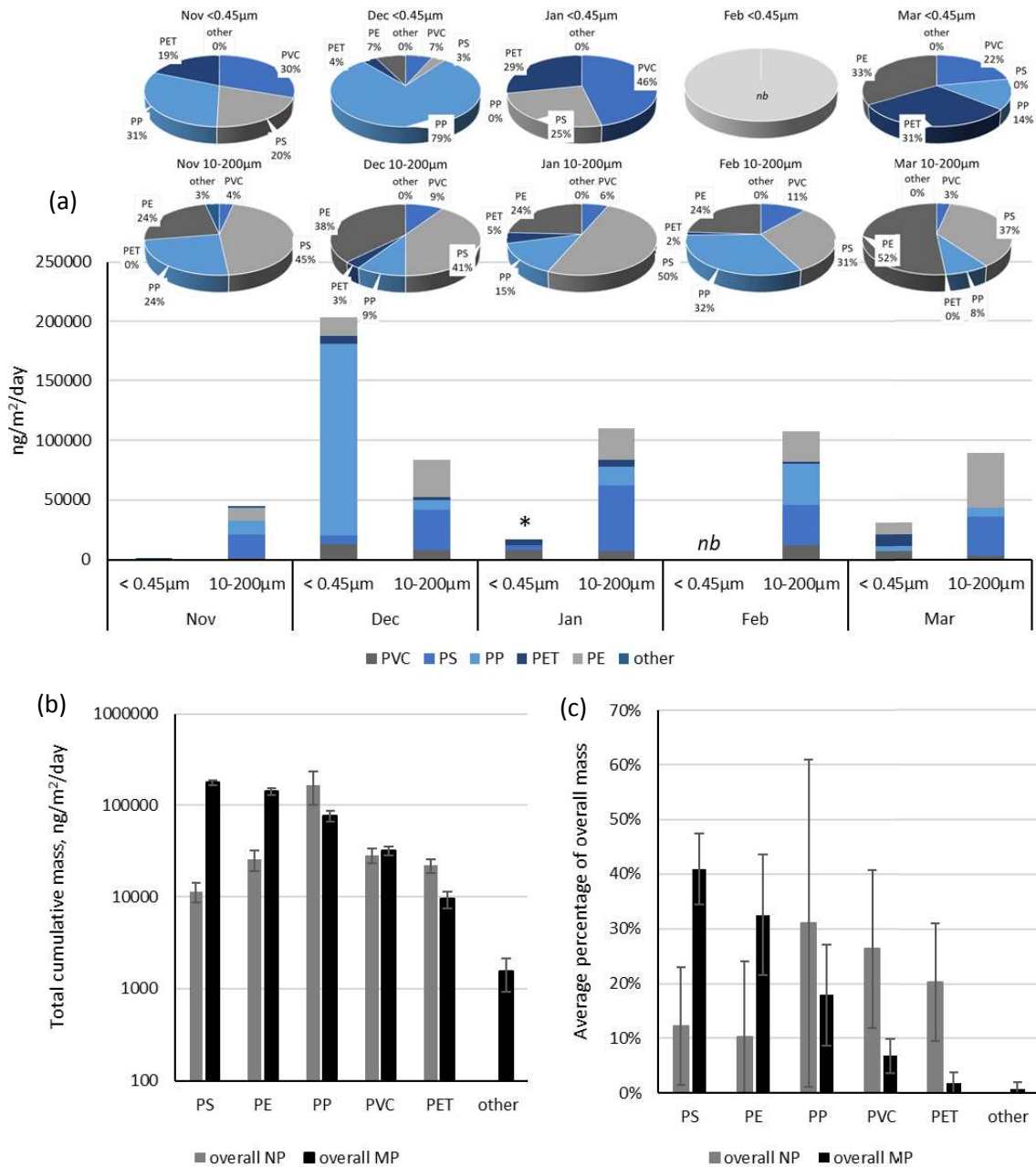
146 Particle counts for MP >10µm were several orders of magnitude lower than that calculated for
 147 NP <0.45µm, as would be expected for comparable mass results for these different particle
 148 size ranges. MP particle counts ranged from 297- 462 particles m⁻² day⁻¹ (average of 365
 149 particles m⁻² day⁻¹) whereas NP estimated particle counts (adopting the conservative particle
 150 size of 0.45µm) ranged from below detection to 43 x10⁸ particles m⁻² day⁻¹ (11x10⁸ particles m⁻²
 151 day⁻¹). This agrees with the increasing particle count relative to decreased particle size found
 152 in both microplastic and nanoplastic studies(Bianco & Passananti, 2020). This suggests that
 153 while comparable mass of MP and NP occur in the atmospheric deposition at this site, a far
 154 greater number of NP particles are being deposited compared to MP.



155
 156 Figure 1. Comparison of NP and MP mass (a), number (b), and the relative number of
 157 particles across samples considering both the analysed MP and NP results (c).

158 To ensure comparability, five of the more frequent polymer types were specifically analysed
 159 (polystyrene-PS, polyethylene-PE, polypropylene-PP, polyvinyl chloride-PVC and
 160 polyethylene terephthalate-PET). Multiple plastic polymer types were found in each sample at
 161 both MP and NP particle size range (Figure 2a). With the exception of the February NP sample
 162 where results were below detection limits, all samples contained PVC as both MP and NP.
 163 Similarly, PET was found in all NP samples (excl. Feb) but was absent in the MP samples for
 164 November and March. Conversely, PE and PP were found in the MP samples for January, but
 165 reported below the limits of detection for NP in the same samples.

166 The overall (cumulative) mass of each plastic type for MP and NP is comparative (Figure 2b),
 167 with greater NP quantities of PVC, PET and PP compared to MP. When compared as a
 168 proportion of the total mass of MP or NP, this differentiation in polymer composition is more
 169 easily visualised, with PS, and PE predominantly occurring as MP, PP occurring in moderate
 170 proportions in both MP and NP particle size ranges, and PVC and PET occurring
 171 predominantly in NP.



172
 173 Figure 2. Types of plastic found in the MP atmospheric deposition and NP deposition. Figure
 174 2(a) presents the mass of each polymer type within each sample relative to the two particle
 175 size groups (NP <0.45µm or MP<10µm), (b) the mass of each polymer type over the total
 176 monitoring period relative to the particle size (NP <0.45µm or MP<10µm), (c) the percentage
 177 of polymer relative to the total MP (or NP) mass. Further information is provided in the
 178 Supplementary information.

179 * denotes the <0.45µm mass of plastic in the January sample after the detection limit is lowered from 80% to 30% accuracy. At
 180 80% both January and February present <0.45µm plastic masses below the detection limit (<10ng/ml). When the accuracy of

181 plastic identification is loosened from an 80% correlation to a 30% correlation (of spectral peaks) then PP, PET and PVC can be
182 identified and quantified in the <0.45µm samples for January.

183 There does not appear to be a direct link between MP and NP polymer type occurrence in this
184 limited dataset, and it is suggested this may be because of the long-distance transport and
185 distal source of MP and NP. The deposited MP and NP may have been transported an
186 extensive distance (100's km) and due to their different particle characteristics may have come
187 from different sources and travelled different distances due to the relative remote location of
188 the sample collection site, and therefore may not be directly related.

189 *MP and NP atmospheric transport*

190 Simple, indicative atmospheric back trajectory and air/particle history modelling can provide a
191 valuable insight into where MP and NP may have been transported from, what elevation in the
192 atmosphere they were transported through, and how far they have travelled. To provide a high
193 level comparative overview of MP and NP atmospheric transport for particles deposited at this
194 Pyrenean field site, long time step atmospheric particle transport modelling was undertaken.
195 This modelling was designed to illustrate the difference in atmospheric transport (extent,
196 elevation) between MP and NP and not to be prescriptive or illustrative of individual sample
197 findings in detail.

198 Controlled environment laboratory examination of the field/laboratory assessed atmospheric
199 settling velocity of MP or NP particles is a new area of research, but early atmospheric
200 modelling has been completed using estimations of MP settling velocities from Stokes Law
201 (S. Allen et al., 2019; Trainic et al., 2020; Wright et al., 2020). Therefore, for the purposes of
202 this discussion, MP settling velocities have been calculated using Stokes Law, to consider the
203 potential atmospheric transport of sampled MP and to compare this to the potential
204 atmospheric transport of newly quantified NP. For simplicity, particles were considered to be
205 cylindrical (acknowledging that fibres or a range of lengths and diameter were found in the MP
206 samples and that NP particle shapes were not defined). For the purposes of this modelling
207 assessment MP particles were defined as 25µm (the predominant size range for the MP
208 particles) and NP as 0.45µm (acknowledging that there will potentially have been greater
209 particle counts for smaller particle sizes in the NP samples). Settling velocities for the 25µm
210 and 0.45µm generic plastic particles were calculated following:

$$211 \quad V_t = \frac{gd^2(\rho_p - \rho_m)}{18\mu}$$

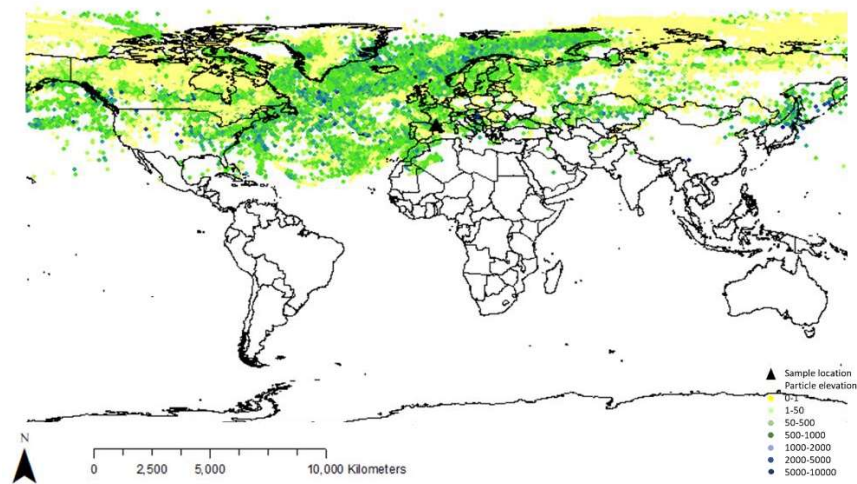
212 Where g is acceleration due to gravity (9.8m s⁻²), ρ_p defines the density of the plastic particle
213 (1g cm⁻³), ρ_d is the density of the medium (air, 1.27 kg/m³ at 5 °C), and μ is the dynamic
214 viscosity of the medium (air, 1.74 x 10⁻⁵ kg m⁻¹ s⁻¹ at 5 °C). Settling velocities were estimated
215 as 0.02m/s for 25µm MP spheres and 6.3 x 10⁻⁶ m s⁻¹ for 0.45µm plastic particles. This results
216 in a simplistic atmospheric transport time (from estimated planetary boundary layer upper
217 elevation of 600m a.g.l.) of 8.5 hours for a 25µm MP particle if no dynamic mixing, turbulence
218 or change in atmospheric conditions occurred during transit. For the smaller particles, this
219 duration extends out past one month (>744hrs). The dynamic mixing, atmospheric
220 characteristics, particle removal due to precipitation (scavenging) and dry deposition therefore
221 potentially have a significant influence on the transport and deposition of these <0.45µm
222 particles.

223 To illustrate the potential influencing area of MP relative to NP, the dynamic HYSPLIT
224 atmospheric transport modelling for the sample particles was completed relative to selected
225 size and settling velocities. Whilst it is clear that the ~ 1 month time step for sampling precludes
226 accurate particle back trajectory analysis for the specific samples, the following analysis was

227 carried out to attempt to elucidate any difference between micro and nano plastics transport
228 and sources.

229 HYSPLIT particle dispersion modelling was undertaken using the HYSPLIT concentration
230 module and particle analysis, backwards modelling the trajectory using both wet and dry
231 deposition for a conservative and illustrative release of 1 particle per hour for a 24hr period,
232 with cyclic emission repeated every 24hours for the duration of the sample period. Particles
233 were parameterised as: MP - 25 μ m (the average MP particle size in the MP dataset), 1g cc⁻¹
234 (Kooi & Koelmans, 2019), settling velocity 0.02m s⁻¹, default wet deposition of in and below
235 cloud wet removal of 8.0E-05 1 s⁻¹ (Draxler & Hess, G, 2018; Stein et al., 2015); NP - 0.45 μ m,
236 1g cc⁻¹ (Kooi & Koelmans, 2019), settling velocity 6.3 x 10⁻⁶ m s⁻¹, cyclic emission of 1particle/hr
237 for 24 hours repeated every 24hours. The resulting particle plots were created to illustrate the
238 extent of particle transport and the elevation (above ground level) relative to the monitoring
239 period (Figure 3). The atmospheric model was capped to 10,000m a.g.l..

(a)



(b)

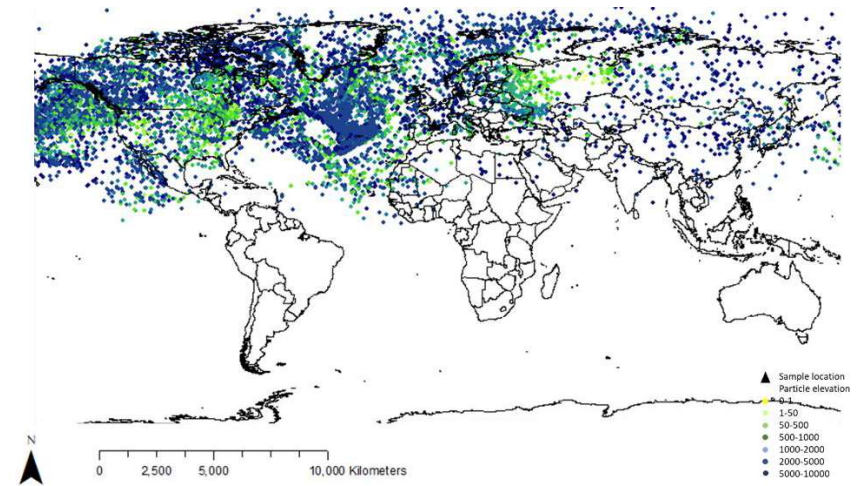
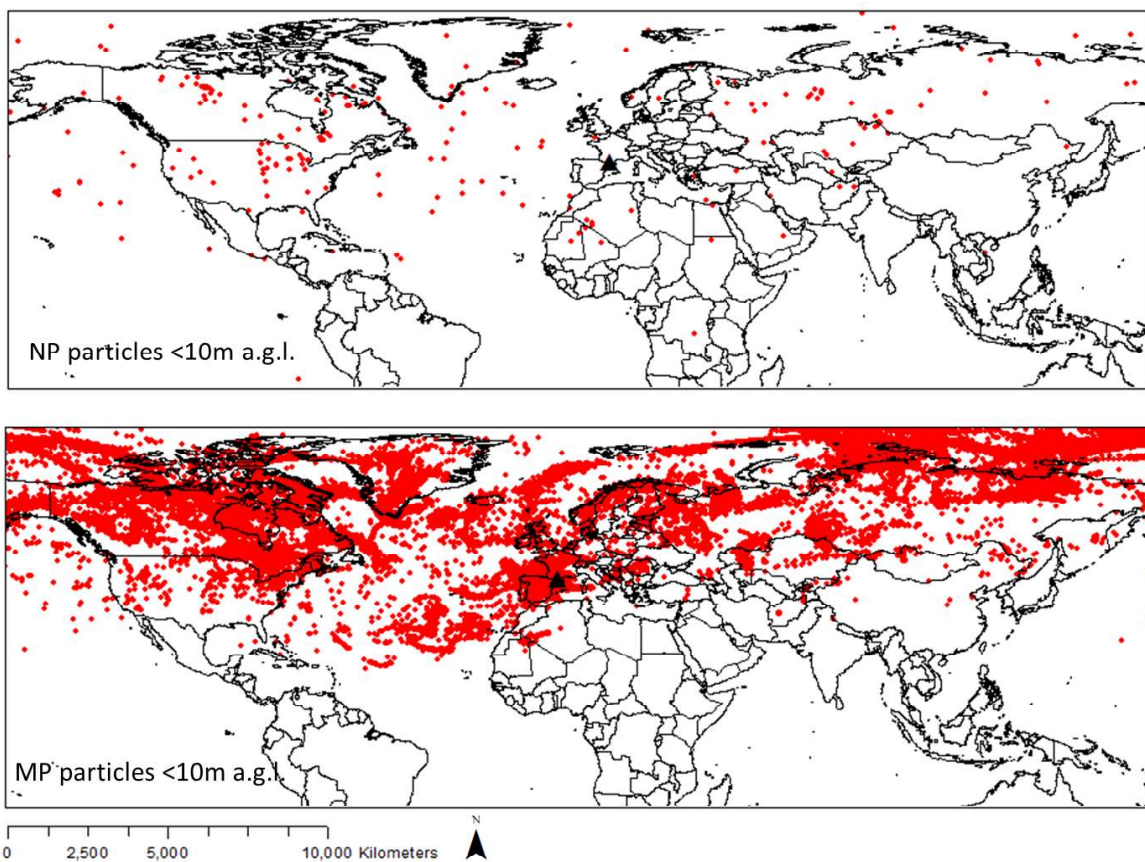


Figure 3. MP (a) and NP (b) particle plot for all sample periods with the respective particle elevation above ground level.

The model outputs identify MP to be transported generally at or below 2000m a.g.l., with particles transport from relatively close to the site (<100km, potentially due to resuspension of previously deposited atmospheric MP) to 10,000km away. The spatial distribution for this high level visualisation of MP particle movement suggests particles to have been transported from and passing over Europe, north America, northern Africa and the Atlantic Ocean. Comparatively, NP particles appear to extend over a greater northern hemisphere spatial

250 distance, extending down the north western (Atlantic) African coast, across China and the
251 north Pacific Ocean and encroaching further into the Atlantic side of the Arctic circle than the
252 modelled MP. NP particles occur through the modelled atmosphere, with notable particles
253 predicted to occur above 2000m a.g.l. compared to very few MP modelled at these higher
254 elevations. NP in general were suggested to travel extended distance (<100km) prior to
255 occurring at the field site, with less occurrence of shorter travel compared to MPs.

256 The model results were disaggregated to try and identify the spatial 'source' areas for MP and
257 NP to this field site using these very general particle parameters and gross sampling
258 conditions. Modelled particle backward trajectories were followed to identify which particles
259 would be found at 'ground level' (0-10m a.g.l. adopted as the surface and entrainment zone),
260 during the sample period (samples November to March 2018). All particles that fell to or below
261 10m a.g.l. were spatially plotted to identify indicative possible source locations for MP and NP
262 for this site using this simple overview model.



263
264 Figure 4. Visualisation of particles at or below 10m a.g.l. during the backward trajectory particle
265 modelling.

266 High quantities of MP were found at or below 10m a.g.l. during the backward trajectory particle
267 modelling, but notably fewer NP were found at this low elevation. The NP are noted to
268 predominantly stay elevated over the modelled duration therefore presenting a lower particle
269 count within the 0-10m a.g.l. 'ground level' illustrated in Figure 4. NP remain elevated for an
270 extended period of time compared to MP, and extend vertically across the entire troposphere
271 (PBL and free troposphere) while MP altitudes are generally lower (<3000m a.g.l.). Both MP
272 and NP backward particle modelling suggests long distance transport, with the majority of
273 particles elevated above ground level close to the sample location (not locally sourced).

274 If the percentage of particles modelled at an elevation of ground level ($\leq 10\text{m a.g.l.}$) are
 1 275 counted, the potential spatial source extents can be tentatively identified (Table 1) (for this
 2 276 sample period at this location). The backward particle modelling can identify possible source
 3 277 areas (through analysis of the location where particles are modelled to be at ground level),
 4 278 however, whether there is a plastic pollution source at the modelled location needs further
 5 279 detailed analysis.

280 Table 1. Potential source areas of MP and NP to this site for the monitored and modelled
 9 281 duration

Microplastic			Nanoplastic					
Location	MP km ⁻²	Potential source*	Location	MP km ⁻²	Potential source*	Location	NP km ⁻²	Potential source*
Spain	0.00602	3%	Germany	0.000142	<1%	Norway	3.34E-06	1%
France	0.005094	3%	Kazakhstan	0.000136	<1%	Afghanistan	3.2E-06	1%
Norway	0.002261	1%	Montenegro	0.000132	<1%	United States	3.04E-06	15%
Andorra	0.001799	<1%	Belarus	8.52E-05	<1%	Kazakhstan	2.73E-06	4%
Canada	0.001395	24%	Mongolia	5.48E-05	<1%	Morocco	2.6E-06	<1%
Portugal	0.001379	<1%	Poland	5.38E-05	<1%	Canada	2.54E-06	18%
Croatia	0.001237	<1%	Kyrgyzstan	4.65E-05	<1%	Mauritania	2.22E-06	1%
Oceans and Seas	0.000120	43%	Hungary	4.53E-05	<1%	Uzbekistan	2.07E-06	<1%
Switzerland	0.000941	<1%	Macedonia	3.64E-05	<1%	Mali	1.88E-06	1%
Iceland	0.000879	<1%	Slovakia	3.35E-05	<1%	Algeria	1.87E-06	2%
Greenland	0.000851	6%	Czech Republic	3.05E-05	<1%	Sweden	1.27E-06	<1%
Finland	0.000806	1%	Belgium	2.57E-05	<1%	Turkey	1.23E-06	<1%
Netherlands	0.000684	<1%	Italy	2.42E-05	<1%	Russia	1.16E-06	15%
Romania	0.000615	<1%	Afghanistan	2.08E-05	<1%	Egypt	1.11E-06	<1%
Denmark	0.000537	<1%	Bulgaria	1.64E-05	<1%	Iran	6.4E-07	<1%
Russia	0.000522	15%	Algeria	1.5E-05	<1%	Greenland	6.05E-07	2%
Bosnia and Herzegovina	0.000414	<1%	Mauritania	1.33E-05	<1%	Saudi Arabia	5.75E-07	<1%
Faroe Islands	0.000393	<1%	Georgia	1.31E-05	<1%	Zaire	5.27E-07	<1%
Ireland	0.000385	<1%	Lithuania	1.09E-05	<1%	Sudan	4.79E-07	<1%
Estonia	0.00031	<1%	Austria	9.96E-06	<1%	Oceans and Seas	2.44E-07	38%
Moldova	0.0002	<1%	Western Sahara	8.33E-06	<1%	China	1.05E-07	<1%
United Kingdom	<1%	<1%	Tajikistan	6.8E-06	<1%			
Sweden	<1%	<1%	Uzbekistan	6.2E-06	<1%			
United States	<1%	2%	Ukraine	5.44E-06	<1%			
Serbia	<1%	<1%	Turkey	4.93E-06	<1%			
Latvia	<1%	<1%	China	3.47E-06	<1%			
Morocco	<1%	<1%	Mali	2.81E-06	<1%			

282 * % of total representative MP and NP particles derived from this location

283 Potential source areas were estimated from model outputs as MP or NP per km² and as a
 284 percentage of all particles $\leq 10\text{m a.g.l.}$. MP or NP per km² provide a spatially comparable
 285 surface 'emission' rate per designated area (country or ocean areas). The percentage values
 286 provide an indicative comparable land mass or ocean specific general contribution to the
 287 overall field site during this sample period. While it is acknowledged this is very indicative and
 288 not directly representative of the field samples, these results provide a first assessment of the
 289 potential gross source areas that may contribute MP and NP to this site.

290 The simplistic model assessment of potential MP and NP source areas suggests continental
 291 Europe (France, Spain, Andorra) and Norway to be key possible areas of MP when source is
 292 considered relative to area (MP km⁻²). When considered as a proportion of the total modelled
 293 MP potentially transported to the field site during this monitored period, the marine
 294 environment (Atlantic Ocean, Mediterranean Ocean) are suggested to be significant
 295 contributors to atmospheric MP (43%). NP appears to be transported from a greater distance,

296 with Norway, south central Asia (Afghanistan), and north America suggested as possible areas
297 of NP contribution. However, when considered by continent or ocean, the marine environment
298 is suggested to a notable contributor to atmospheric NP at this site (38%), similar to MP model
299 outputs (D. Allen et al., 2022; S. Allen et al., 2020). It is noted that a much greater number of
300 NP particles would be expected for $\leq 10\text{m a.g.l.}$ if the model was extended backward in time
301 (if the backward particle trajectories were run for long enough to follow particle down to lower
302 atmospheric elevations) rather than being constrained to the monitored duration of the field
303 samples. However, for small NP this could be weeks or more and would change for each
304 particle depending on its trajectory and environmental conditions, resulting in a highly complex
305 and extensive dataset that is not considered appropriate for the overview transport modelling
306 intended to support the MP and NP field findings in this study.

307 **Conclusion**

308 This study presents a direct comparison of NP and MP content in atmospheric deposition
309 samples collected in a relatively remote area of the Pyrenees, France. While MP is analysed
310 by particle and NP is analysed by mass, using simple volume to mass calculations a
311 comparison has been made of both mass and particle count for MP and NP for this monitoring
312 period. NP ($<0.45\mu\text{m}$) were found to present a comparative mass compared to MP in the same
313 sample, and a correspondingly much higher particle count (NP \gg MP particles per sample).
314 The MP and NP sample composition varies, with plastic polymer predominance in the MP
315 particle size range not directly reflected in the NP proportion of the sample. This may be due
316 to the atmospheric transport dynamics of the different particle sizes, acknowledging the
317 smaller NP particles fall within the realms of Brownian motion. The long distance transport
318 necessary to create MP and NP at this sample location may also influence the sample
319 composition, suggesting that NP may have been transported from more extensive distances
320 from the site than MP particles. The HYSPLIT back trajectories illustrate the global long range
321 atmospheric transport of nanoplastic and give indications of the possible source areas. Most
322 notably the ocean is illustrated as the source of $\sim 38\%$ of global atmospheric emissions of
323 nanoplastics. This finding suggests that whilst previous work has shown the ocean as a source
324 for MP, it is also clearly the source of a much greater amount of nanoplastic, and as such
325 requires urgent investigation.

327 **Declaration of Competing Interest**

328 The authors declare they have no competing interest

330 **Supplementary materials**

331 Supplementary Dataset (xls)

332 Supplementary Information

333

334

335 **References**

- 1
2 336 Akoueson, F., Chbib, C., Monchy, S., Paul-Pont, I., Doyen, P., Dehaut, A., & Duflos, G.
3 337 (2021). Identification and quantification of plastic additives using pyrolysis-GC/MS: A
4 338 review. *Science of the Total Environment*, 773.
5 339 <https://doi.org/10.1016/j.scitotenv.2021.145073>
6
7 340 Allen, D., Allen, S., Jickells, T., Abassi, S., Baker, A., Bergmann, M., Brahney, J., Butler, T.,
8 341 Dusan, M., Eckhart, S., Kanakidou, M., Laj, P., Levermore, J., Li, D., Liss, P., Liu, K.,
9 342 Majowald, N., Masque, P., Mayes, A., ... Duce, R. (2022). The Atmospheric Cycle of
10 343 Microplastics in the Marine Environment. *Nature Reviews Earth & Environment*, (in
11 344 review).
12
13 345 Allen, S., Allen, D., Baladima, F., Phoenix, V. R., Thomas, J. L., Le Roux, G., & Sonke, J. E.
14 346 (2021). Evidence of free tropospheric and long-range transport of microplastic at Pic du
15 347 Midi Observatory. *Nature Communications*. [https://doi.org/10.1038/s41467-021-27454-](https://doi.org/10.1038/s41467-021-27454-7)
16 348 [7](https://doi.org/10.1038/s41467-021-27454-7)
17
18 349 Allen, S., Allen, D., Moss, K., Le Roux, G., Phoenix, V. R., & Sonke, J. (2020). Examination
19 350 of the ocean as a source for atmospheric microplastics. *PLoS ONE*, 15(5), e0232746.
20 351 <https://doi.org/10.1371/journal.pone.0232746>
21
22 352 Allen, S., Allen, D., Phoenix, V. R., Le Roux, G., Duranteza, P., Simonneau, A., Stéphane,
23 353 B., & Galop, D. (2019). Atmospheric transport and deposition of microplastics in a
24 354 remote mountain catchment. *Nature Geoscience*, 12, 339–344.
25 355 <https://doi.org/10.1038/s41561-019-0335-5>
26
27 356 Ambrosini, R., Azzoni, R. S., Pittino, F., Diolaiuti, G., Franzetti, A., & Parolini, M. (2019). First
28 357 evidence of microplastic contamination in the supraglacial debris of an alpine glacier.
29 358 *Environmental Pollution*, 253, 297–301. <https://doi.org/10.1016/j.envpol.2019.07.005>
30
31 359 Banerjee, A., & Shelver, W. L. (2021). Micro- and nanoplastic induced cellular toxicity in
32 360 mammals: A review. *Science of the Total Environment*, 755, 142518.
33 361 <https://doi.org/10.1016/j.scitotenv.2020.142518>
34
35 362 Bergmann, M., Gutow, L., & Klages, M. (2015). Marine anthropogenic litter. In M. Bergmann,
36 363 L. Gutow, & M. Klages (Eds.), *Marine Anthropogenic Litter* (1st ed.). Springer Open.
37 364 <https://doi.org/10.1007/978-3-319-16510-3>
38
39 365 Bergmann, M., Mützel, S., Primpke, S., Tekman, M. B., Trachsel, J., & Gerdt, G. (2019).
40 366 White and wonderful? Microplastics prevail in snow from the Alps to the Arctic. *Science*
41 367 *Advances*, 5(8), eaax1157. <https://doi.org/10.1126/sciadv.aax1157>
42
43 368 Bianco, A., & Passananti, M. (2020). Atmospheric Micro and Nanoplastics : An Enormous
44 369 Microscopic Problem. *Sustainability*, 12, 7327. <https://doi.org/10.3390/su12187327>
45
46 370 Brahney, J., Hallerud, M., Heim, E., Hahnenbergere, M., & Sukumaran, S. (2020). Plastic
47 371 rain in protected areas of the United States. *Science*, 368(6496), 1257–1260.
48 372 <https://doi.org/10.1126/science.aaz5819>
49
50 373 Cabrera, M., Valencia, B. G., Lucas-Solis, O., Calero, J. L., Maisincho, L., Conicelli, B.,
51 374 Massaine Moulatlet, G., & Capparelli, M. V. (2020). A new method for microplastic
52 375 sampling and isolation in mountain glaciers: A case study of one antisana glacier,
53 376 Ecuadorian Andes. *Case Studies in Chemical and Environmental Engineering*,
54 377 2(September), 100051. <https://doi.org/10.1016/j.cscee.2020.100051>
55
56 378 Deng, Y., Yan, Z., Shen, R., Wang, M., Huang, Y., Ren, H., Zhang, Y., & Lemos, B. (2020).
57 379 Microplastics release phthalate esters and cause aggravated adverse effects in the
58 380 mouse gut. *Environment International*, 143, 105916.

- 381 <https://doi.org/10.1016/j.envint.2020.105916>
- 1
2 382 Draxler, R. R., & Hess, G. D. (2018). *Description of the Hysplit4 modeling system*.
3 383 [https://www.researchgate.net/publication/255682850_Description_of_the_HYSPLIT_4_](https://www.researchgate.net/publication/255682850_Description_of_the_HYSPLIT_4_modelling_system)
4 384 [modelling_system](https://www.researchgate.net/publication/255682850_Description_of_the_HYSPLIT_4_modelling_system)
- 5
6 385 Ferreira, I., Venâncio, C., Lopes, I., & Oliveira, M. (2019). Nanoplastics and marine
7 386 organisms: What has been studied? *Environmental Toxicology and Pharmacology*,
8 387 67(November 2018), 1–7. <https://doi.org/10.1016/j.etap.2019.01.006>
- 9
10 388 Feynman, R. (1963). *Brownian motion*. Feynman Lectures.
11 389 https://www.feynmanlectures.caltech.edu/l_41.html
- 12
13 390 Frias, J. P. G. L., & Nash, R. (2019). Microplastics: Finding a consensus on the definition.
14 391 *Marine Pollution Bulletin*, 138(November 2018), 145–147.
15 392 <https://doi.org/10.1016/j.marpolbul.2018.11.022>
- 16
17 393 Gigault, J., El Hadri, H., Nguyen, B., Grassl, B., Rowenczyk, L., Tufenkji, N., Feng, S., &
18 394 Wiesner, M. (2021). Nanoplastics are neither microplastics nor engineered
19 395 nanoparticles. *Nature Nanotechnology*, 16(5), 501–507. [https://doi.org/10.1038/s41565-](https://doi.org/10.1038/s41565-021-00886-4)
20 396 [021-00886-4](https://doi.org/10.1038/s41565-021-00886-4)
- 21
22 397 Gonçalves, J. M., & Bebianno, M. J. (2021). Nanoplastics impact on marine biota: A review.
23 398 *Environmental Pollution*, 273. <https://doi.org/10.1016/j.envpol.2021.116426>
- 24
25 399 Huang, J. N., Wen, B., Zhu, J. G., Zhang, Y. S., Gao, J. Z., & Chen, Z. Z. (2020). Exposure
26 400 to microplastics impairs digestive performance, stimulates immune response and
27 401 induces microbiota dysbiosis in the gut of juvenile guppy (*Poecilia reticulata*). *Science*
28 402 *of the Total Environment*, 733, 138929. <https://doi.org/10.1016/j.scitotenv.2020.138929>
- 29
30 403 Huntington, A., Corcoran, P. L., Jantunen, L., Thaysen, C., Bernstein, S., Stern, G. A., &
31 404 Rochman, C. M. (2020). A first assessment of microplastics and other anthropogenic
32 405 particles in Hudson Bay and the surrounding eastern Canadian Arctic waters of
33 406 Nunavut. *Facets*, 5(1), 432–454. <https://doi.org/10.1139/FACETS-2019-0042>
- 34
35 407 Joachim, C. (2005). To be nano or not to be nano? *Nature Materials*, 4(2), 107–109.
36 408 <https://doi.org/10.1038/nmat1319>
- 37
38 409 Kim, S.-K., Lee, H.-J., Kim, J.-S., Kang, S.-H., Yang, E.-J., Cho, K.-H., Tian, Z., & Andradý,
39 410 A. (2021). Importance of Seasonal Sea Ice in the Western Arctic Ocean to the Arctic
40 411 and Global Microplastic Budgets. *Journal of Hazardous Materials*.
41 412 <https://doi.org/10.1016/j.jhazmat.2021.125971>
- 42
43 413 Kooi, M., & Koelmans, A. A. (2019). Simplifying Microplastic via Continuous Probability
44 414 Distributions for Size, Shape, and Density. *Environmental Science and Technology*
45 415 *Letters*, 6(9), 551–557. <https://doi.org/10.1021/acs.estlett.9b00379>
- 46
47 416 Li, B., Ding, Y., Cheng, X., Sheng, D., Xu, Z., Rong, Q., Wu, Y., Zhao, H., Ji, X., & Zhang, Y.
48 417 (2020). Polyethylene microplastics affect the distribution of gut microbiota and
49 418 inflammation development in mice. *Chemosphere*, 244, 125492.
50 419 <https://doi.org/10.1016/j.chemosphere.2019.125492>
- 51
52 420 Li, T., & Raizen, M. G. (2013). Brownian motion at short time scales. *Annalen Der Physik*,
53 421 525(4), 281–295. <https://doi.org/10.1002/andp.201200232>
- 54
55 422 Liu, S., Wu, X., Gu, W., Yu, J., & Wu, B. (2020). Influence of the digestive process on
56 423 intestinal toxicity of polystyrene microplastics as determined by in vitro Caco-2 models.
57 424 *Chemosphere*, 256, 127204. <https://doi.org/10.1016/j.chemosphere.2020.127204>
- 58
59 425 Materić, D., Kasper-Giebl, A., Kau, D., Anten, M., Greilinger, M., Ludewig, E., van Sebille, E.,
60
61
62
63
64
65

- 426 Röckmann, T., & Holzinger, R. (2020). Micro- and nanoplastics in Alpine snow – a new
1 427 method for chemical identification and quantification in the nanogram range.
2 428 *Environmental Science & Technology*, 54(5), 2353–2359.
3 429 <https://doi.org/10.1021/acs.est.9b07540>
4
- 5 430 Materic, D., Kjær, H. A., Vallenga, P., Tison, J.-L., Rockmann, T., & Holzinger, R. (2022).
6 431 Nanoplastics measurements in Northern and Southern polar ice. *Environmental*
7 432 *Research*, 208, 112741. <https://doi.org/10.1016/j.envres.2022.112741>
8
- 9 433 Materić, D., Ludewig, E., Brunner, D., Rochmann, T., & Holzinger, R. (2021). Nanoplastics
10 434 transport to the remote, high-altitude Alps. *Environmental Pollution*, 288(117697).
11 435 <https://doi.org/10.1016/j.envpol.2021.117697>
12
- 13 436 Menges, F. (2018). *Spectragryph* (v1.2.8). <https://www.ffmpeg2.de/spectragryph/index.html>
14
- 15 437 Mitrano, D. M., Wick, P., & Nowack, B. (2021). Placing nanoplastics in the context of global
16 438 plastic pollution. *Nature Nanotechnology*, 1–10. [https://doi.org/10.1038/s41565-021-](https://doi.org/10.1038/s41565-021-00888-2)
17 439 [00888-2](https://doi.org/10.1038/s41565-021-00888-2)
18
- 19 440 Munno, K., Frond, H. De, Donnell, B. O., & Rochman, C. M. (2020). Increasing the
20 441 accessibility for characterizing microplastics : Introducing new application-based and
21 442 spectral libraries of plastic particles (SLoPP & SLoPP-E). *Analytical Chemistry*, 92(3),
22 443 2443–2451. <https://doi.org/10.1021/acs.analchem.9b03626>
23
- 24 444 Okoffo, E. D., Ribeiro, F., O'Brien, J. W., O'Brien, S., Tschärke, B. J., Gallen, M.,
25 445 Samanipour, S., Mueller, J. F., & Thomas, K. V. (2020). Identification and quantification
26 446 of selected plastics in biosolids by pressurized liquid extraction combined with double-
27 447 shot pyrolysis gas chromatography–mass spectrometry. *Science of the Total*
28 448 *Environment*, 715(January), 136924. <https://doi.org/10.1016/j.scitotenv.2020.136924>
29
- 30 449 Piccardo, M., Renzi, M., & Terlizzi, A. (2020). Nanoplastics in the oceans: Theory,
31 450 experimental evidence and real world. *Marine Pollution Bulletin*, 157(April), 111317.
32 451 <https://doi.org/10.1016/j.marpolbul.2020.111317>
33
- 34 452 Pimpke, S., Cross, R. K., Mintenig, S. ., Simon, M., Vianello, A., Gerdt, G., & Vollertsen, J.
35 453 (2020). Toward the Systematic Identification of Microplastics in the Environment:
36 454 Evaluation of a New Independent Software Tool (siMPle) for Spectroscopic Analysis.
37 455 *Applied Spectroscopy*, 74(9), 1127–1138. <https://doi.org/10.1177/0003702820917760>
38
- 39 456 Rubio, L., Marcos, R., & Hernández, A. (2020). Potential adverse health effects of ingested
40 457 micro- and nanoplastics on humans. Lessons learned from in vivo and in vitro
41 458 mammalian models. *Journal of Toxicology and Environmental Health - Part B: Critical*
42 459 *Reviews*, 23(2), 51–68. <https://doi.org/10.1080/10937404.2019.1700598>
43
- 44 460 Stein, A. F., Draxler, R. R., Rolph, G. D., Stunder, B. J. B., Cohen, M. D., & Ngan, F. (2015).
45 461 NOAA's HYSPLIT Atmospheric Transport and Dispersion Modeling System. *Bulletin of*
46 462 *the American Meteorological Society*, 96(12), 2059–2077.
47 463 <https://doi.org/10.1175/BAMS-D-14-00110.1>
48
- 49 464 Trainic, M., Flores, J. M., Pinkas, I., Pedrotti, M. L., Lombard, F., Bourdin, G., Gorsky, G.,
50 465 Boss, E., Rudich, Y., Vardi, A., & Koren, I. (2020). Airborne microplastic particles
51 466 detected in the remote marine atmosphere. *Communications Earth & Environment*,
52 467 1(1), 1–9. <https://doi.org/10.1038/s43247-020-00061-y>
53
- 54 468 Wahl, A., Le Juge, C., Davranche, M., El Hadri, H., Grassl, B., Reynaud, S., & Gigault, J.
55 469 (2021). Nanoplastic occurrence in a soil amended with plastic debris. *Chemosphere*,
56 470 262. <https://doi.org/10.1016/j.chemosphere.2020.127784>
57
- 58 471 Wright, S. L., & Kelly, F. J. (2017). Plastic and Human Health: A Micro Issue? *Environmental*
59
60
61
62
63
64
65

472 *Science and Technology*, 51(12), 6634–6647. <https://doi.org/10.1021/acs.est.7b00423>

1
2 473 Wright, S. L., Ulke, J., Font, A., Chan, K. L. ., & Kelly, F. J. (2020). Atmospheric microplastic
3 474 deposition in an urban environment and an evaluation of transport. *Environment*
4 475 *International*, 136, 105411. <https://doi.org/10.1016/j.envint.2019.105411>

5
6 476 Xu, J. L., Thomas, K. V., Luo, Z., & Gowen, A. A. (2019). FTIR and Raman imaging for
7 477 microplastics analysis: State of the art, challenges and prospects. *TrAC - Trends in*
8 478 *Analytical Chemistry*, 119, 115629. <https://doi.org/10.1016/j.trac.2019.115629>

9
10 479 Yang, H., Lai, H., Huang, J., Sun, L., Mennigen, J. A., Wang, Q., Liu, Y., Jin, Y., & Tu, W.
11 480 (2020). Polystyrene microplastics decrease F-53B bioaccumulation but induce
12 481 inflammatory stress in larval zebrafish. *Chemosphere*, 255.
13 482 <https://doi.org/10.1016/j.chemosphere.2020.127040>

14
15 483 Yang, T., Luo, J., & Nowack, B. (2021). Characterization of Nanoplastics, Fibrils, and
16 484 Microplastics Released during Washing and Abrasion of Polyester Textiles.
17 485 *Environmental Science and Technology*, 55(23), 15873–15881.
18 486 <https://doi.org/10.1021/acs.est.1c04826>

19
20 487 Yee, M. S. L., Hii, L. W., Looi, C. K., Lim, W. M., Wong, S. F., Kok, Y. Y., Tan, B. K., Wong,
21 488 C. Y., & Leong, C. O. (2021). Impact of microplastics and nanoplastics on human
22 489 health. *Nanomaterials*, 11(2), 1–23. <https://doi.org/10.3390/nano11020496>

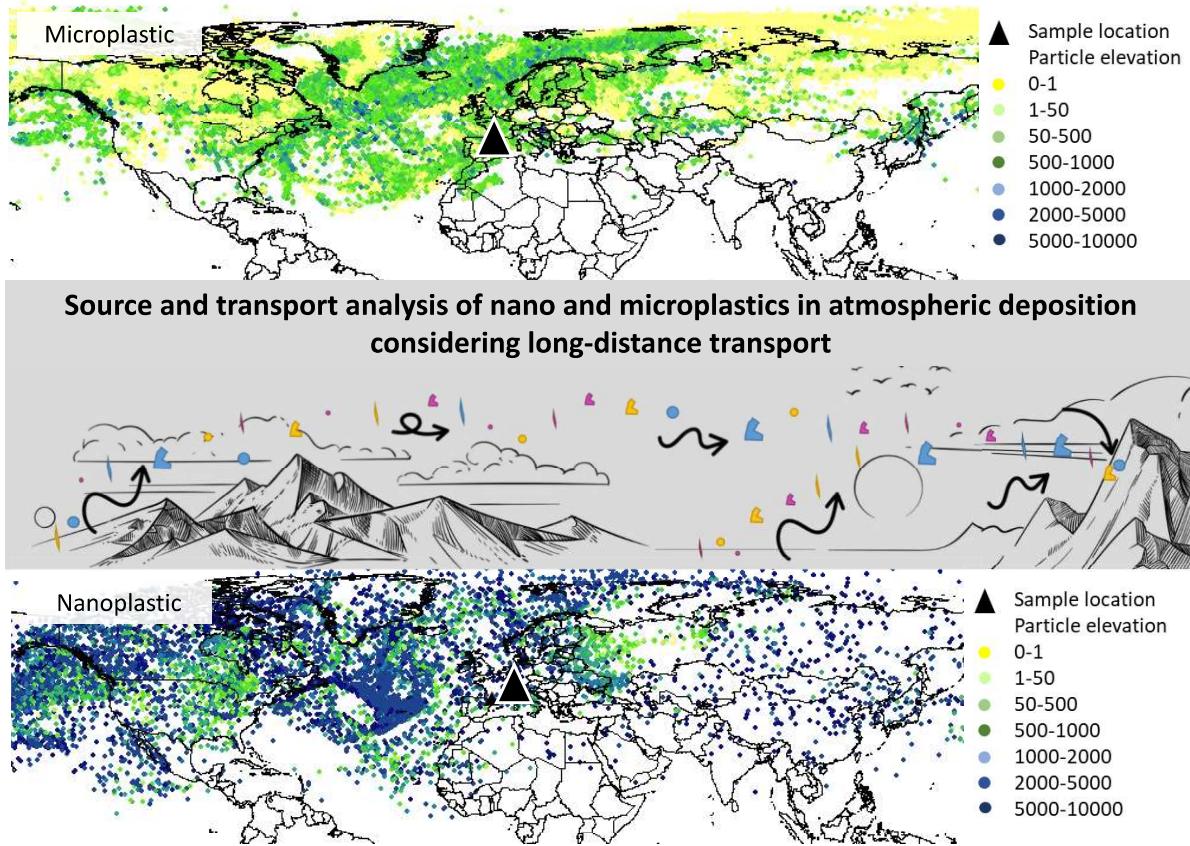
23
24 490 Zheng, Y., Li, J., Sun, C., Cao, W., Wang, M., Jiang, F., & Ju, P. (2021). Comparative study
25 491 of three sampling methods for microplastics analysis in seawater. *Science of the Total*
26 492 *Environment*, 765, 144495. <https://doi.org/10.1016/j.scitotenv.2020.144495>

27
28 493
29
30
31
32
33
34
35
36
37
38
39
40
41
42
43
44
45
46
47
48
49
50
51
52
53
54
55
56
57
58
59
60
61
62
63
64
65

Highlights

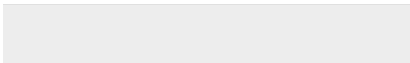
- Comparable micro and nanoplastic assessment is vital to advancing source-transport-fate assessments.
- There are effective methods to compare atmospheric micro and nanoplastics
- Comparative analysis suggests order of magnitude greater nanoplastic particles in the atmosphere
- Nanoplastics are transported further and across a greater altitude range
- Tentative global source assessment of atmospheric micro(nano)plastics

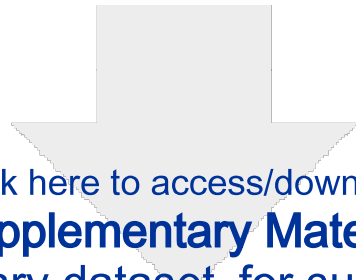
Graphical Abstract



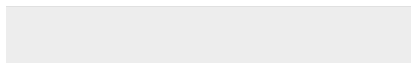
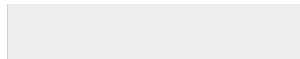


Click here to access/download
Supplementary Material
Supplementary Information.docx





Click here to access/download
Supplementary Material
Supplementary dataset_for submission.xlsx





Click here to access/download
Supplementary Material
Statement of Novelty.docx



Acknowledgments

The authors would like to thank the Ocean Frontiers Institute (OFI) for the support of Steve Allen through the International Postdoctoral Fellowship, the Leverhulme Trust, grant ECF-2019-306, for their support of Deonie Allen and the EPSRC doctoral scholarship provided to Anna MacDonald. The authors acknowledge the support provided to Gael Le Roux by the ANR-20-CE34-0014 Atmo-Plastic project, the Plasticopyr project within the Interreg V-A Spain-France- Andorra programme, the CNRS TRAM Project and ANR-15-CE01-0008, Observatoire Homme- Milieu Pyrénées Haut Vicdessos - LABEX DRIIHM ANR-11-LABX0010. The authors also acknowledge the support from Dutch Research Council (Nederlandse Organisatie voor Wetenschappelijk Onderzoek – NWO) projects: “Nanoplastics: hormone-mimicking and inflammatory responses?” (grant number OCENW.XS2.078) and “Size distribution of nanoplastics in indoor, urban and rural air” (grant number OCENW.XS21.2.042) provided to Dušan Materić.